Mass Spectrometry Reveals Differences in Stability and Subunit Interactions between Activated and Nonactivated Conformers of the $(\alpha\beta\gamma\delta)_4$ Phosphorylase Kinase Complex*[S]

Laura A. Lane‡§, Owen W. Nadeau¶, Gerald M. Carlson¶, and Carol V. Robinson‖**

Phosphorylase kinase (PhK), a 1.3 MDa enzyme complex that regulates glycogenolysis, is composed of four copies each of four distinct subunits (α, β, γ, and δ). The catalytic protein kinase subunit within this complex is γ, and its activity is regulated by the three remaining subunits, which are targeted by allosteric activators from neuronal, metabolic, and hormonal signaling pathways. The regulation of activity of the PhK complex from skeletal muscle has been studied extensively; however, considerably less is known about the interactions among its subunits, particularly within the non-activated *versus* activated forms of the complex. Here, nanoelectrospray mass spectrometry and partial denaturation were used to disrupt PhK, and subunit dissociation patterns of non-activated and phospho-activated (autophosphorylation) conformers were compared. In so doing, we have established a network of subunit contacts that complements and extends prior evidence of subunit interactions obtained from chemical crosslinking, and these subunit interactions have been modeled for both conformers within the context of a known three-dimensional structure of PhK solved by cryoelectron microscopy. Our analyses show that the network of contacts among subunits differs significantly between the nonactivated and phospho-activated conformers of PhK, with the latter revealing new interprotomeric contact patterns for the β subunit, the predominant subunit responsible for PhK's activation by phosphorylation. Partial disruption of the phosphorylated conformer yields several novel subcomplexes containing multiple β subunits, arguing for their self-association within the activated complex. Evidence for the theoretical $\alpha\beta\gamma\delta$ protomeric subcomplex, which has been sought but not previously observed, was also derived from the phospho-activated complex. In addition to changes in subunit interaction patterns upon phospho-activation, mass spectrometry revealed a large change in the overall stability of the complex, with the phospho-activated conformer being more labile, in concordance with previous hypotheses on the mechanism of allosteric activation of PhK through perturbation of its inhibitory quaternary structure. ***Molecular & Cellular Proteomics 11: 10.1074/mcp.M112.021394, 1768–1776, 2012.***

In the cascade activation of glycogenolysis in skeletal muscle, phosphorylase kinase (PhK),[1] upon becoming activated through phosphorylation, subsequently phosphorylates glycogen phosphorylase in a Ca^{2+}-dependent reaction. This phosphorylation of glycogen phosphorylase activates its phosphorolysis of glycogen, leading to energy production (1). The 1.3 MDa $(\alpha\beta\gamma\delta)_4$ PhK complex was the first protein kinase to be characterized and is among the largest and most complex enzymes known (2). As such, the intact complex has proved to be refractory to high resolution x-ray crystallographic or NMR techniques; however, low resolution structures of the nonactivated and Ca^{2+}-saturated conformers of PhK have been deduced through modeling (3) and solved by means of three-dimensional electron microscopic (EM) reconstruction (4–7), and they show that the complex is a bilobal structure with interconnecting bridges. Approximate locations of small regions of each subunit in the complex are known (8–10) and show that the subunits pack head-to-head as apparent $\alpha\beta\gamma\delta$ protomers that form two octameric $(\alpha\beta\gamma\delta)_2$ lobes associating in D_2 symmetry (11), although direct evidence that the $\alpha\beta\gamma\delta$ protomers are discrete, functional subcomplexes has been lacking until now.

Approximately 90% of the mass of the PhK complex is involved in its regulation. Its kinase activity is carried out by the catalytic core of the γ subunit (44.7 kDa), with the k_{cat} being enhanced up to 100-fold by multiple metabolic, hormo-

From the ‡Department of Chemistry, University of Cambridge, Lensfield Road, Cambridge CB2 1EW, UK; §Department of Chemistry, Chemistry Research Laboratory, Mansfield Road, Oxford OX1 3TA, UK; ¶Department of Biochemistry and Molecular Biology, University of Kansas Medical Center, Kansas City, Kansas 66160; ‖Department of Chemistry, the Physical and Theoretical Chemistry Laboratory, University of Oxford, South Parks Road, Oxford, OX1 3QZ, UK

Received June 14, 2012, and in revised form, August 24, 2012
⌘ *Author's Choice*—Final version full access.
Published, MCP Papers in Press, September 10, 2012, DOI 10.1074/mcp.M112.021394

[1] The abbreviations used are: EM, electron microscopy; γCRD, γ subunit C-terminal regulatory domain; nES, nanoelectrospray; PhK, phosphorylase kinase.

nal, and neural stimuli that are integrated through allosteric sites on PhK's three regulatory subunits, α, β, and δ (12). The small δ subunit (16.7 kDa), which is tightly bound integral calmodulin (13), binds to at least the C-terminal regulatory domain of the γ subunit (γCRD) (14, 15), thereby mediating activation of the catalytic subunit by the obligate activator Ca^{2+} (16). The α and β subunits, as deduced from DNA sequencing, are polypeptides of 1237 and 1092 amino acids, respectively, with calculated masses prior to post-translational modifications of 138.4 and 125.2 kDa (17, 18). Both subunits can be phosphorylated by numerous protein kinases, including cAMP-dependent protein kinase and PhK itself (2). The α and β subunits are also homologous (38% identity and 61% similarity); however, each subunit has unique phosphorylatable regions that contain nearly all the phosphorylation sites found in these subunits (17, 18).

The regulation of PhK activity by both Ca^{2+} (19–23) and phosphorylation has been studied extensively (reviewed in Ref. 24); however, only the structural effects induced by Ca^{2+} are well characterized (25), primarily through comparison of the non-activated and Ca^{2+}-activated conformers using three-dimensional EM reconstructions (4), small angle x-ray scattering modeling (3), and biophysical (26–28) and chemical crosslinking methods (29–32). In contrast to the Ca^{2+}-activated *versus* non-activated conformers, there are no reported structures of phosphorylated PhK to compare against the non-activated form. A very small amount of structural information for phospho-activated PhK derived from chemical crosslinking raises the possibility of phosphorylation-dependent communication between the β and γ subunits: Arg-18 in the N-terminal phosphorylatable region of β was found to be relatively near the γCRD (33). Several lines of evidence suggest that transduction of the activating phosphorylation signal in PhK occurs concomitantly with conformational changes in β (33) that are detected *via* various methods (10, 34), including chemical crosslinking (35). For example, crosslinking of only the phosphorylated conformer by the short-span crosslinker 1,5-difluoro-2,4-dinitrobenzene results in the formation of β homodimers (35). Correspondingly, more recent two-hybrid screens of the full length β subunit against itself yielded positive binding interactions only for point mutants in which the N-terminal phosphorylatable serine residues were mutated to phosphomimetic glutamates (33). It should be noted, however, that both chemical crosslinking and two-hybrid screening have potential drawbacks in the study of subunit interactions within a multisubunit complex. In the case of the latter, it is difficult when observing homodimeric two-hybrid interactions to determine whether they correspond to naturally occurring interactions between two like subunits within a complex or between two interacting regions within a single subunit of that complex. Studying subunit interactions in a complex through chemical crosslinking comes with its own inherent limitations. For example, an initial mono-derivatization can potentially cause a conformational change in one subunit that might affect the subsequent crosslinking reaction. This is particularly the case if the crosslinker contains a functionality, such as an aromatic group, that can unexpectedly direct it to a specific locus on the protein complex (36, 37). In addition, the spacer arms on many crosslinkers are sufficiently long to confound interpretation as to whether two subunits within a complex are actually in contact. Similarly, it should be proved that any observed crosslinked conjugate is formed from subunits within a complex, as opposed to between complexes (38, 39), a control that is often not run. Thus, it is prudent to analyze subunit interactions within a complex using a variety of approaches.

To corroborate, complement, and expand the previous two-hybrid screening and chemical crosslinking studies of PhK's subunit interactions and to investigate changes in the pattern of subunit interactions induced by phosphorylation, we carried out comparative MS analyses of both intact and partially denatured forms of nonactivated and phospho-activated PhK using mass spectrometers modified specifically to enhance the transmission of large noncovalently bound protein complexes (40–42). The array of subunit interactions detected for the nonactivated PhK complex largely replicated those reported in the crosslinking literature for this conformer, both corroborating those earlier studies and validating the use of these MS approaches to study subunit interactions within the PhK complex. Additionally, several novel subcomplexes of PhK were revealed, most notably an $\alpha\beta\gamma\delta$ protomer, which corroborates the observed packing of this subcomplex in the D_2 symmetrical $(\alpha\beta\gamma\delta)_4$ native complex (9, 11). Moreover, we show herein that the array of subunit interactions detected for phospho-activated PhK differs significantly from that observed for the nonactivated conformer, with only the former showing extensive self-interactions between and among the regulatory β subunits. As is discussed, this suggests that activation through phosphorylation is associated with increased interprotomeric interactions in the bridged core of the PhK complex (33, 35).

EXPERIMENTAL PROCEDURES

Proteins—Nonactivated PhK was purified from the psoas muscle of female New Zealand White rabbits as described elsewhere (43). The enzyme was stored at −80 °C in 50 mM HEPES buffer (pH 6.8, 10% w/v sucrose, and 0.2 mM EDTA). Phospho-activated PhK was prepared via autophosphorylation essentially as described (43), resulting in a 40-fold activation of phosphorylase conversion at pH 6.8. Nonactivated PhK was incubated at 30 °C for 20 min in 50 mM HEPES (pH 8.2) containing ATP (1.2 mM), Ca^{2+} (0.2 mM), $Mg(CH_3CO_2)_2$ (10 mM), and EGTA (0.1 mM). The reaction was quenched by the addition of excess EDTA (25 mM final concentration). Phospho-PhK was then purified *via* size exclusion chromatography over Sepharose 6B, concentrated to 1.45 mg/ml by ultrafiltration using an Amicon Ultra-2 (3 kDa) concentration device, and stored in 50 mM β-glycerophosphate buffer (pH 6.8, 10% w/v sucrose, and 2 mM EDTA). The extent of the incorporation of phosphate into the α and β subunits of PhK was determined using ^{32}P-labeled ATP as described elsewhere (33).

Sample Preparation for MS—Nonactivated and phospho-activated PhK (0.13 and 0.08 nmole, respectively) were buffer-exchanged into

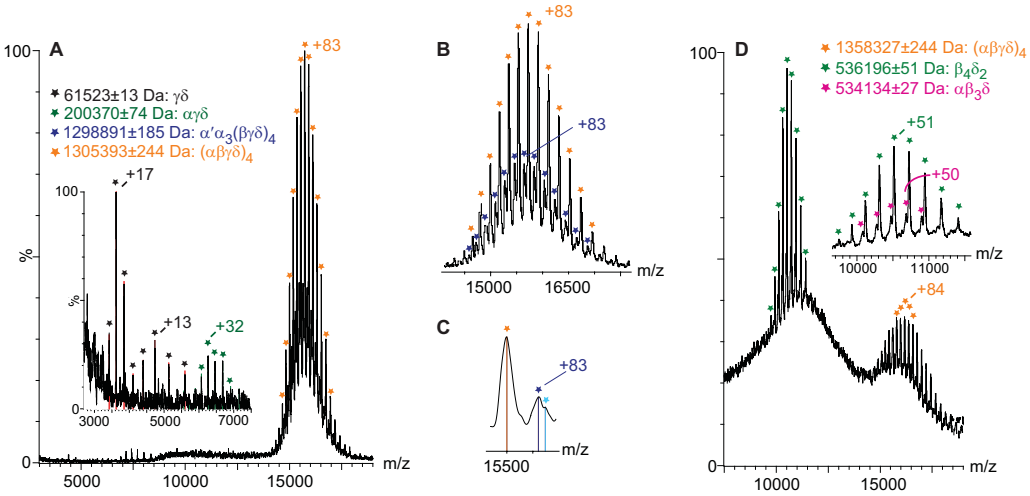

FIG. 1. **Top-down MS of nonactivated and phospho-activated PhK.** *A*, mass spectrum of intact, nonactivated $(\alpha\beta\gamma\delta)_4$ PhK in 50 mM ammonium acetate (*orange*), with two less intense but well-resolved series corresponding to the $\alpha\gamma\delta$ trimer (*green*) and the $\gamma\delta$ dimer (*black*). *B*, magnification of the charge state series (*orange*) corresponding to the intact complex, but showing an additional, less intense partially overlapping charges state series (*dark blue*) that is consistent in terms of mass with the intact complex, in which one α subunit is replaced by a lower mass splice variant, termed α' (52). *C*, discrete shoulders (*light blue*) shown in a magnified view of two peaks at 15,500 *m/z* from the intact PhK charge series suggesting the possible substitution of more than one molecule of α' for α in the hexadecameric complex. *D*, nanoelectrospray mass spectrum of intact phospho-activated $(\alpha\beta\gamma\delta)_4$ PhK (*orange*), with two partially resolved charge series (magnified in *inset*) corresponding to $\beta_4\delta_2$ (*green*) and $\alpha\beta_3\delta$ subcomplexes (*pink*).

50 mM ammonium acetate (pH 6.8) using a Vivaspin (5 kDa) column (Vivascience, Hannover, Germany) and concentrated to ~30 μl. To generate subcomplexes of the enzyme *via* partial denaturation (44), the pH levels of the solutions were adjusted by means of dilution with either ammonium hydroxide (10% to 20%: v/v) or acetic acid (10% to 20%: v/v). The final pH values measured were 9.9 (10% ammonium hydroxide), 10.2 (20% ammonium hydroxide), 3.0 (10% acetic acid), and 2.7 (20% acetic acid). Unless otherwise stated, partial denaturants were typically incubated with protein samples at room temperature for 5 min prior to MS analyses.

Nanoelectrospray MS—Nondenaturing nanoelectrospray (nES) mass spectra were acquired on a Q-ToF 2 mass spectrometer (Micromass/Waters, Milford, MA), modified for high mass detection (42), or on a Qstar XL (MDS Sciex, Applied Biosystems, Carlsbad, CA) using a previously described protocol optimized for the transmission of noncovalent protein complexes (41). Analysis of PhK on the Qstar XL instrument was carried out in positive ion mode using the following general parameters: ion spray voltage, 1.4 kV; declustering potential, 100 V and 15 V; focusing potential, 100 V; quadrupole voltage, 150 V; collision gas, 12; ion release delay, 6; and ion release width, 5. Experiments were performed with a collision cell pressure of ~11.8 mbar. The following experimental parameters were applied in positive ion mode for the analysis of intact phospho-PhK on the Q-time-of-flight 2 instrument: capillary voltage, 1.7 kV; sample cone, 194 V; extraction cone, 5 V; collision energy, 200 V; collision cell pressure, 20 mbar; hexapole ion guide pressure, 42 mbar; analyzer pressure, 1.5×10^{-4} mbar; backing pressure, 1.0 mbar; and ToF pressure, 2.1×10^{-6} mbar.

LC/MS Analyses of PhK Conformers—Capillary high pressure LC/MS analyses of individual PhK and phospho-PhK subcomplexes were carried out using an LC-Packings Ultimate System (Dionex, Sunnyvale, CA) equipped with a capillary UV detector set at 214 and 280 nm. Samples were prepared in a 1:1 (v/v) solution of 0.1% TFA, and 1 μl of sample was applied to a capillary polystyrene-divinylbenzene reverse-phase monolithic column (200 μm inner diameter × 5 cm; Dionex) equilibrated at 90% solvent A (0.05% TFA) and 10% solvent B (0.04% TFA, 90% acetonitrile). A linear gradient of solvent B (10% to 70%) was developed over 25 min using a flow rate of 3 μl/min. The column effluent was analyzed via nES MS using a Q-star Pulsar (ABI/Sciex, Sunnyvale, CA) mass spectrometer.

Data Analyses—Spectra were acquired and processed using MassLynx v4.1 (Waters, Manchester, UK) and Analyst QS (MDS Sciex, Applied Biosystems). Errors are reported as ±1 standard deviation. All spectra were calibrated externally using a 100 mg/ml solution of cesium iodide. All spectra are shown with minimal smoothing and without background subtraction. Subcomplex compositions were determined using the iterative search algorithm SUMMIT (45).

RESULTS

MS Analyses of the Intact 1.3 MDa Complex of Nonactivated PhK—To compare subunit interactions in the two PhK conformers, we first established conditions for measuring the intact $(\alpha\beta\gamma\delta)_4$ complexes *via* MS from nondenaturing solutions (41, 44). nES MS of native, nonactivated PhK revealed a predominant and well-resolved charge state series centered on a +83 charge state, with an experimental mass ($mass_{EXP}$) of 1,305,393 ± 244 Da, which corresponds to the partially solvated $(\alpha\beta\gamma\delta)_4$ hexadecameric form of the complex (Fig. 1*A*). The measured mass exceeds the theoretical mass ($mass_{THEO}$ = 1,298,994 Da) of PhK by 6388 Da; this mass difference likely reflects buffer and water molecules associated with the protein complex (46), a phenomenon of the soft ionization process required to observe biological complexes in the gas phase (47). In addition to the intact $(\alpha\beta\gamma\delta)_4$ complex, $\alpha\gamma\delta$ ($mass_{THEO}$ = 199,664 Da) and $\gamma\delta$ ($mass_{THEO}$ = 61,339 Da) subcomplexes were detected at lower *m/z* values by measurements for two well-resolved charge state series that corresponded, respectively, to masses of 200,370 ± 74

and 61,573 ± 13 Da. Corroborating these results, both subcomplexes have been observed previously after dissociation of the PhK complex with high concentrations of LiBr (48, 49).

Close inspection of the charge series for the intact complex (Fig. 1*B*, *orange*) revealed an additional charge series (Fig. 1*B*, *dark blue*) corresponding to an intact hexadecameric complex in which one α subunit is replaced by a lower mass splice variant of this subunit (α'), an isoform found predominately in slow twitch oxidative skeletal muscle (50, 51). Alternative splicing of the α subunit results in an internal deletion and loss of residues 654–712 (52), with a corresponding mass loss of 6414 Da. The experimental mass difference of 6370 Da (0.69% error) measured between $\alpha'\alpha_3(\beta\gamma\delta)_4$ ($mass_{THEO}$ = 1,292,580 Da) and the $(\alpha\beta\gamma\delta)_4$ complex is in close agreement. Multiple substitutions of α' for α in other complexes are suggested by discrete shoulders observed in the second charge series (Fig. 1*C*); however, these were not resolved sufficiently for accurate mass calculations.

MS Analyses of the Intact 1.3 MDa Complex of Phospho-activated PhK—Analysis *via* nondenaturing nES MS of the phospho-PhK conformer revealed three significant charge state series (Fig. 1*D*). The first, ranging approximately between 15,000 and 17,000 *m/z* values and centering on the +83 charge state, yielded a measured mass of 1,358,327 ± 211 Da, which corresponds to the intact, partially solvated, phosphorylated $(\alpha\beta\gamma\delta)_4$ complex. The phosphorylation of the complex resulted in the incorporation of 3.9 and 2.2 mol -PO_3 per α and β subunit, respectively (see Experimental Procedures), for a total of 24.4 mol -PO_3 per $(\alpha\beta\gamma\delta)_4$ complex. The 1927 Da additional mass from the -PO_3 groups raises the $mass_{THEO}$ of the complex to 1,300,921 Da, with the mass difference between the calculated and experimental values again attributed to retention of small molecules. In comparison with native PhK, the broader peaks observed for the phospho-PhK spectrum are consistent with the increased level of heterogeneity associated with phosphorylation of the complex (reviewed in Ref. 24). The second charge series observed for the phospho-conformer was centered on a +51 charge state at ~11,000 Da (Fig. 1*D*), with a measured mass of 536,196 ± 51 Da (Fig. 1*D inset, green stars*). After evaluating all possible combinations of subunits, we found that the subcomplex most closely corresponding to this series in terms of mass is a $\beta_4\delta_2$ hexamer ($mass_{THEO}$ = 533,728 Da). In addition, a less intense third series in the same *m/z* range corresponded by mass ($mass_{EXP}$ = 534,134 ± 27 Da) to an $\alpha\beta_3\delta$ subcomplex having a theoretical mass of 530,272 Da (Fig. 1*D inset, pink*). As is discussed further on, both of these novel subcomplexes containing three and four β subunits indicate that the β subunits must occupy the core of the bridged bilobal dimer of $(\alpha\beta\gamma\delta)_2$ octameric lobes that describe PhK (5, 9, 11). Moreover, the detection of subcomplexes comprising primarily the β subunits in the mass spectrum of only phospho-PhK is consistent with previous reports demonstrating homodimeric crosslinking of β only with phosphorylated forms of PhK (35, 53).

TABLE I

Calculated and observed masses of intact complexes of PhK and subcomplexes generated from the $(\alpha\beta\gamma\delta)_4$ complex by either solution disruption with partial denaturants or CID

Complexes and subcomplexes	Theoretical mass (Da)	Experimental mass (Da)
$(\alpha\beta\gamma\delta)_4$	1,298,994	1,305,393 ± 24
$\alpha'\alpha_3(\beta\gamma\delta)_4$	1,292,580	1,298,891 ± 19
$\beta_4\delta_2$	533,730	536,196 ± 51
$\alpha\beta_3\delta$	530,275	534,134 ± 27
$\alpha\beta\beta$	388,494	390,819 ± 30
$\alpha\beta\gamma\delta$	324,749	326,892 ± 87
$\alpha\beta\delta$	280,106	281,562 ± 20
$\alpha\beta$	263,410	264,730 ± 58
$\beta\beta$	250,169	251,368 ± 59
$\alpha\gamma\delta$[a]	199,664	201,148 ± 81
$\alpha\gamma$	182,968	183,522 ± 70
$\beta\gamma$	169,727	170,409 ± 69
$\alpha\delta$	155,021	155,698 ± 32
$\beta\delta$	141,780	142,365 ± 40
$\gamma\gamma$	89,286	89,569 ± 64
$\gamma\delta$	61,339	61,523 ± 13

[a] Stable $\alpha\gamma\delta$ subcomplexes have been isolated after expression in insect cells (58) and after dissociation of the $(\alpha\beta\gamma\delta)_4$ complex with LiBr (48).

When the mass spectra of non-activated and phospho-activated PhK were compared, we found that the highest intensity charge state peaks from the latter corresponded to its subcomplexes, whereas with the nonactivated conformer, the intact complex accounted for the most intense charge state peaks. This difference implies that the phospho-activated complex is more labile than its nonactivated counterpart. Similarly, the activated conformer of PhK produced by Ca^{2+}-saturation is increasingly labile to thermal perturbation relative to the native, nonactivated conformer (27). The above two results are consistent with the oft postulated view that the activity of the native, nonactivated conformer of PhK is under extreme quaternary constraint and that perturbation of its quaternary structure leads to activation or, more specifically, deinhibition (33, 54). It should be noted, however, that the subunits in all forms of the complex remain tightly associated under standard solution conditions (*i.e.*, buffer and low salt) and do not readily dissociate (see Ref. 55 and references therein).

Subcomplexes Formed from the Native, Nonactivated $(\alpha\beta\gamma\delta)_4$ PhK Complex—Manipulating the pH enabled us to disassemble the native, nonactivated PhK hexadecamer into subcomplexes (Table I) and individual subunits (Table II). Disruption occurred more readily at low pH values. The addition of acetic acid (final concentration 10% v/v) to PhK in 50 mM ammonium acetate (pH 6.8) yielded individual α (139,063 ± 27 Da), β (125,602 ± 33 Da), and γ (44,724 ± 14 Da) subunits, as well as two subcomplexes corresponding to an $\alpha\beta$ dimer (264,730 ± 58 Da) and an $\alpha\beta\delta$ trimer (281,562 ± 199 Da) (Fig. 2*A*). This association of the three regulatory subunits (α, β,

TABLE II
Calculated and observed masses of the subunits of PhK
masses for the large α and β regulatory subunits were determined via CID, and masses for γ and δ were determined *via* LC/MS.

Subunits	Theoretical mass (Da)	Experimental mass (Da)	
		Nonactivated PhK	Phospho-activated PhK
α	138,325	138,792 ± 40	139,358 ± 47
β	125,084	125,602 ± 33	125,660 ± 30
γ	44,643	44,667 ± 0.8	44,669 ± 3.0
δ	16,696	16,787 ± 0.3	16,784 ± 7.2

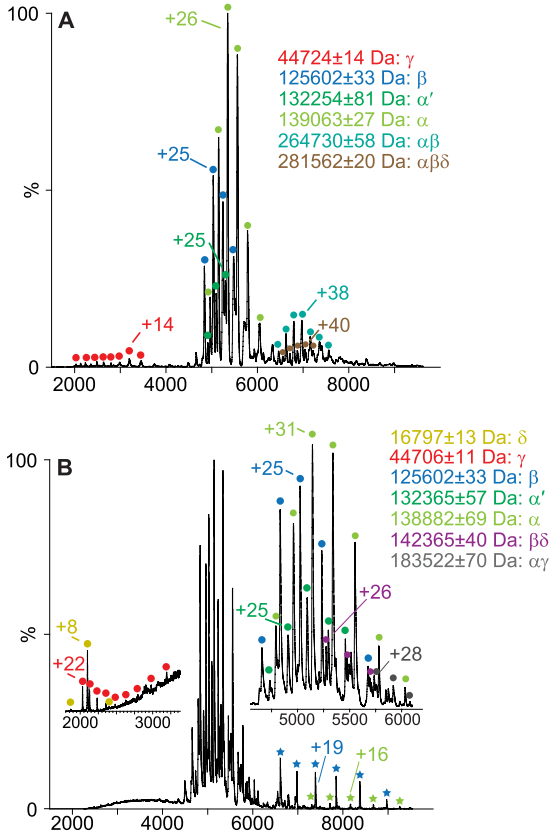

FIG. 2. **Nanoelectrospray mass spectra of partially denatured, nonactivated PhK.** *A*, spectrum of PhK acquired in 10% (v/v) acetic acid. *B*, spectrum acquired for PhK under solution conditions identical to those described under *A*, but with activating MS conditions. Inset represents a magnified view of the major charge series peak. *Green* and *blue stars* in the full spectrum indicate ions corresponding to low-charge "stripped" α and β subunits, respectively. Low *m/z* (200–3000) inset shows charge series corresponding to the small γ and δ subunits.

and δ) with one another in the absence of the catalytic γ subunit has not previously been observed in, or suggested by, other approaches and was unexpected, given that each of these three regulatory subunits is known to directly interact with the γ subunit (33). A low intensity charge series centered on a +38 charge state ($mass_{EXP}$ = 132,254 ± 58 Da) between 6000 and 8000 *m/z* corresponds well to a splice variant of α (52) termed α' ($mass_{THEO}$ = 131,893 Da), which is present in minor quantities in preparations of PhK from rabbit psoas muscle (50).

Further analyses of subunit contacts in the non-activated conformer were carried out by altering either parameters governing the MS activation (Fig. 2*B*) or the acidic solution disruption conditions (supplemental Fig. S1). Regarding the former, we further analyzed subunit contacts in the complex by using more energetic gas phase ion activation conditions to promote dissociation of the complex under the same slightly acidic solution conditions as described above. Gas phase activation in an argon-filled collision cell results in the ejection of a coulombically unfolded, highly charged monomer (ejected species) from a dimer or higher order oligomer, resulting in a relatively low-charged "stripped" oligomer missing one subunit (56). For the most part, the dissociation of oligomers *via* this process is asymmetric (40). As shown in Fig. 2*B*, such activation was evidenced by detectable levels of stripped α and β subunits (*green* and *blue stars*, respectively), each revealed by a greater extent of desolvation and a lower charge state (+16 and +19, respectively) than observed for α (+31) and β (+25) under less activating conditions (Fig 2*B*, *inset*). The small δ subunit was also observed at low *m/z* values (Fig. 2*B*, *low m/z inset*). Additionally, two new species corresponding to $\alpha\gamma$ ($mass_{EXP}$ = 183,522 ± 70 Da) and $\beta\delta$ ($mass_{EXP}$ = 142,365 ± 40 Da) dimers were detected. In contrast to MS activation of the complex, increasing the final concentration of acetic acid to 20% (v/v) while retaining the original lower energy MS activation parameters yielded a distinct charge series that corresponded to a $\beta\gamma$ subcomplex ($mass_{EXP}$ = 170,409 ± 69 Da) (Table I and supplemental Fig. S1). In summary, of the six heterodimeric subcomplexes that are theoretically possible upon disruption of the $(\alpha\beta\gamma\delta)_4$ complex, the only one not observed with disassembly of the non-activated PhK conformer was the $\alpha\delta$ dimer.

To probe further for potential direct interactions between the α and δ subunits within the PhK complex, we selected, using tandem MS, an activated charge state series corresponding to the $\alpha\gamma\delta$ trimer, which happened to overlap the spectrum for the $\alpha\gamma$ dimer. As described above for activation of PhK, CID of the $\alpha\gamma\delta$ and $\alpha\gamma$ heteromers in the collision cell of the tandem MS provides an alternative mechanism to probe for subunit interactions in these subcomplexes by following the production of ejected and stripped species from each subcomplex (40). The pathways of dissociation for both subcomplexes are shown schematically from a tandem MS spectrum of the corresponding charge series isolated at 5196 *m/z* from a 10% v/v ammonium hydroxide solution of PhK (Fig. 3), with full details described under supplemental Fig. S2. Activation of $\alpha\gamma\delta$ by CID revealed two pathways resulting from the ejection of either the catalytic γ subunit (44,702 ± 17 Da) or the δ subunit (16,869 ± 23 Da) to form, respectively, the corresponding stripped $\alpha\delta$ (155,698 ± 32 Da) or $\alpha\gamma$ (183,580 ± 41 Da) subcomplexes (Table I). The results of CID analyses show that the α subunit interacts directly with both

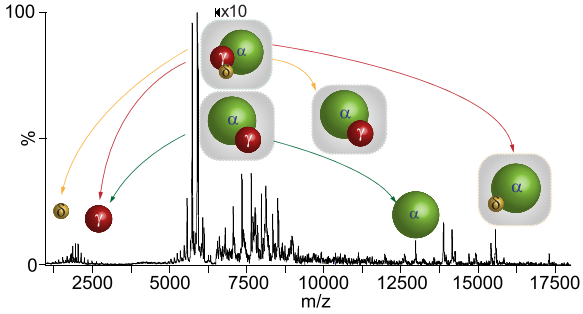

FIG. 3. **Nanoelectrospray tandem mass spectrum of PhK in 10% v/v ammonium hydroxide obtained from mass selection of $\alpha\gamma\delta$ and $\alpha\gamma$ subcomplexes at 5916 *m/z*.** Because of the proximity of their subcomplex mass series, both the $\alpha\gamma\delta$ trimer and the $\alpha\gamma$ dimer were isolated for analysis by CID. The two CID pathways detected for $\alpha\gamma\delta$ are shown by *red* and *yellow arrows* depicting, respectively, asymmetric ejection of γ and δ to form stripped $\alpha\delta$ and $\alpha\gamma$ subcomplexes. The CID pathway of dissociation for $\alpha\gamma$ is depicted by *green arrows*.

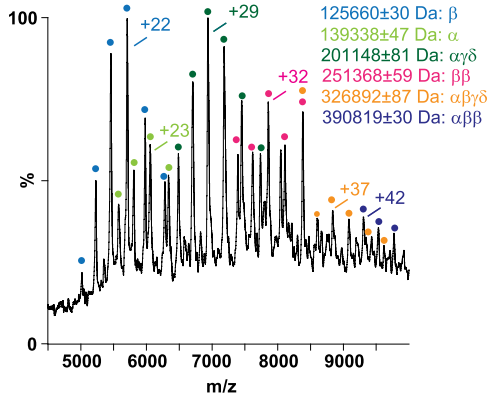

FIG. 4. **Nanoelectrospray mass spectrum of phospho-activated PhK.** Both subunits and subcomplexes were observed in the presence of 10% (v/v) ammonium hydroxide.

the catalytic γ subunit and the δ subunit. Consequently, all six theoretically possible heterodimers are observed, indicating that each subunit interacts with the remaining three, forming an extensive communication network in the nonactivated form of PhK.

Subcomplexes Formed from the Phospho-activated PhK Complex—Unlike in the situation with nonactivated PhK, the detection of subcomplexes was readily achieved with its phospho-activated counterpart, with the use of only minimal amounts of either acidic or basic denaturants (not exceeding 10% total volume). This ease of partial dissociation provides further evidence that the phospho-activated complex is more labile than the nonactivated conformer. The subcomplexes and individual subunits observed with the addition of acetic acid (supplemental Fig. S3*A*) or ammonium hydroxide (Fig. 4 and supplemental Fig. S3*B*) to phospho-activated PhK were in many cases identical to those observed upon disruption of the native, nonactivated conformer. Several new species were observed, however, most notably an intact $\alpha\beta\gamma\delta$ protomer (326,892 ± 87 Da) (Fig. 4, *orange dots*). The observation of this subcomplex represents the first direct evidence of this tetramer within the quaternary structure of PhK. Two additional species, an $\alpha\beta_2$ trimer (390,819 ± 30 Da) and a β_2 dimer (251,368 ± 59 Da), are consistent with the $\alpha\beta_3\delta$ and $\beta_4\delta_2$ subcomplexes observed in MS of the intact phospho-activated PhK complex (Fig. 1*D*). It is important to note that no subcomplexes containing more than one β subunit were obtained from the nonactivated conformer of PhK.

DISCUSSION

MS methods designed for optimal transmission and analyses of large macromolecular assemblies have previously proved successful in determining the stoichiometry and subunit architecture of large multisubunit complexes in the MDa mass range (56). These MS methods complement structural information for such complexes obtained from chemical crosslinking (45). An advantage of these MS methods over crosslinking is that large subcomplexes can usually be unambiguously identified *via* MS (46), whereas crosslinking of large protein complexes to capture oligomeric conjugates contained within is generally less selective, resulting in the formation of a continuum of crosslinked subunits that is sometimes too complex to adequately fractionate and analyze components (39). Consequently, crosslinking is usually most accurate when identifying small product conjugates, such as dimers (39). Our MS results with the nonactivated conformer of PhK show that all but one ($\alpha\alpha$) of the dimeric subunit–subunit interactions identified in a large body of crosslinking literature were observed in either solution disruption or CID experiments (Table I). These similar findings both corroborate the pertinent previous crosslinking results and validate the MS approaches used herein to analyze subunit interactions within the PhK complex; however, one superiority of the top-down MS approaches over crosslinking is evident when comparing the nonactivated to the activated conformers of PhK. Although both approaches readily show differences in subunit interaction maps, the difference in stability of the two complexes is shown only by MS.

The observation of the $\alpha'\alpha_3(\beta\gamma\delta)_4$ subcomplex has implications regarding hetero-oligomeric interactions and tissue-dependent isoform expression. PhK containing the α subunit is found in fast twitch skeletal muscle, whereas the alternatively spliced α' species, in which one exon is deleted (52), is found in PhK from slow twitch oxidative or cardiac muscle (50). That both subunit types can be found within the same subcomplex (Fig. 1*B*) indicates a lack of selectivity for PhK's quaternary structure by tolerating such heterogeneity. It would also seem to indicate that both subunits are simultaneously expressed in certain muscle cells, unless in a solution of purified PhK there can be exchange of α and α' subunits between $(\alpha\beta\gamma\delta)_4$ and $(\alpha'\beta\gamma\delta)_4$ complexes. There is clearly a small number of red fiber types in our source of "white" muscle (*i.e.*, the presence of α'); however, there is no published evidence of subunit exchange involving the α subunit. In fact, even when the α

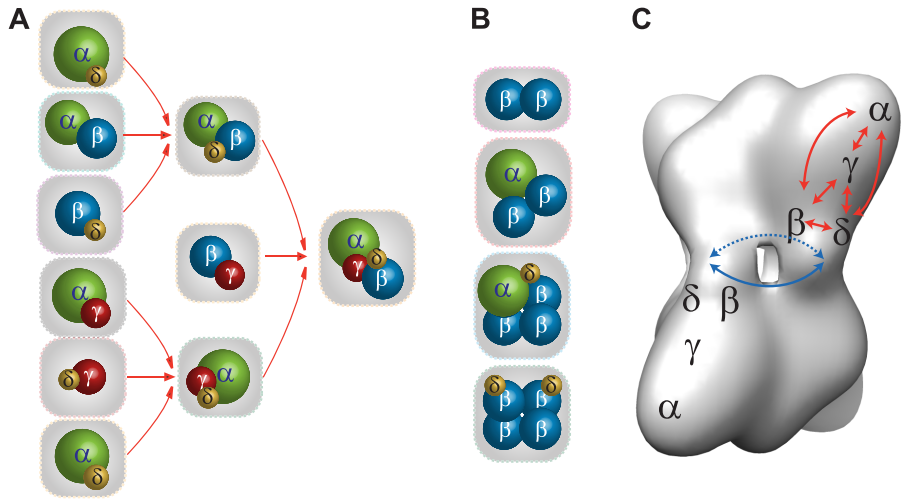

FIG. 5. **Comparison of subunit interaction networks determined for nonactivated and phospho-activated PhK.** *A*, connectivity among the subunits within the $\alpha\beta\gamma\delta$ protomer deduced by detection of heteromeric complexes. *B*, subcomplexes detected only in phospho-activated PhK that show interprotomeric interactions mediated by the β subunits in the $(\alpha\beta\gamma\delta)_4$ complex. *C*, as determined previously by EM methods (8–10), the approximate placement of the four subunits is shown for two $\alpha\beta\gamma\delta$ protomers that are located on opposite $(\alpha\beta\gamma\delta)_2$ lobes of the cryoEM density map of PhK (5). The *red* and *blue arrows* indicate, respectively, subunit interaction networks determined by top-down MS among α, β, γ, and δ subunits in a protomer and the β subunits from each of four protomers in the bridge region of PhK.

subunit is extensively proteolyzed, its fragments remain tightly bound as part of the PhK complex (57). Consequently, it seems likely that both α and α' are synthesized in some cells and that both can simultaneously occur within the same hexadecameric PhK complex.

Several large hetero-oligomeric subcomplexes containing single copies of each subunit, including an $\alpha\gamma\delta$ trimer and an $\alpha\beta\gamma\delta$ tetramer, were observed in mass spectra of the intact and solution disrupted forms of the PhK complex; these indicate extensive subunit communication networks, as well as distinct substructures within PhK's quaternary structure (33). Based on the stoichiometry and positions of the subunits (8–10), the PhK complex has been suggested to comprise four $\alpha\beta\gamma\delta$ protomers that pack as head-to-head pairs to form two long (176 Å) $(\alpha\beta\gamma\delta)_2$ octameric lobes that perpendicularly associate with D_2 symmetry through four central interconnecting bridges (11). Our results herein provide the first direct evidence for such an $\alpha\beta\gamma\delta$ protomer, suggesting that it is a structural and functional moiety in the complex (11). Given the large axial ratio (length/width $>$ 2.3) of the lobes (4) and the peripheral locations (8, 9) and relatively small masses of the γ and δ subunits, we presume that most of the heterodimers identified through chemical crosslinking and our MS analyses reflect subunit contacts within individual $\alpha\beta\gamma\delta$ protomers. If this is true, then the six observed heterodimers ($\alpha\beta$, $\alpha\gamma$, $\alpha\delta$, $\beta\gamma$, $\beta\delta$, $\gamma\delta$), the maximal possible theoretical number, would suggest a localized, but extensive, set of protein–protein interactions in which each subunit interacts with the remaining three within its protomer. The various subcomplexes observed in this study are depicted in Fig. 5, in which the extensive interactions among all the subunits are shown in the context of a three-dimensional cryoEM reconstruction of the non-activated PhK complex (Fig. 5*C*). The trimeric $\alpha\gamma\delta$ subcomplex detected in spectra of intact native PhK and solution disrupted forms of the kinase is an expected dissociation product, as this stable subcomplex has been observed previously (48).

Within the $(\alpha\beta\gamma\delta)_4$ complex, there is considerable evidence of a Ca^{2+}-dependent communication network involving the α, γ, and δ (calmodulin) subunits. For instance, binding of Ca^{2+} to δ causes a mass redistribution on the $(\alpha\beta\gamma\delta)_2$ lobe tips (4) where the carboxy-terminal region of α has been localized (9), and it also alters proteolysis of α near its carboxy-terminus (32). Moreover, the catalytic activities of $(\alpha\beta\gamma\delta)_4$ and $\alpha\gamma\delta$ are stimulated in parallel by Ca^{2+} (49, 58). There is strong indirect evidence that the effects on α of the binding of Ca^{2+} to δ are mediated by γ, specifically by the γCRD, and adjacent regions of its primary structure have been shown to interact with α and δ within PhK. The question of whether a direct δ–α interaction also occurs that could potentially participate in this $\delta \leftrightarrow \gamma \leftrightarrow \alpha$ communication network has not been addressed, because previous evidence for α–δ interactions has been indirect and weak. For example, crosslinking of PhK by several reagents results in the formation of conjugates that correspond by apparent mass to $\alpha\delta$ dimers but crossreact only with an antibody against the α subunit (30, 37), presumably because the epitope on the δ subunit is masked by crosslinking. CID of the $\alpha\gamma\delta$ complex has shown unequivocally for the first time a direct interaction between the α and δ subunits, and together with the other evidence above, this demonstrates that all three subunits interact with one another in the $\alpha\gamma\delta$ subcomplex, and presumably within the $\alpha\beta\gamma\delta$ protomeric structures, of PhK.

One of the primary reasons for performing this work was to determine whether changes in subunit interactions could be

observed upon activation of PhK by phosphorylation. Using electron microscopy (4) and small-angle x-ray scattering (3), it has been established that activation of the nonphosphorylated enzyme by the binding of Ca^{2+} causes structural changes in both its lobes and bridges, but it has not been known whether related structural changes occur upon activation of PhK by phosphorylation. Because any relatively small subcomplex containing more than two of a given subunit (*e.g.*, $\alpha\beta_3\delta$ and $\beta_4\delta_2$) must, by definition, contain the bridged core connecting PhK's two $(\alpha\beta\gamma\delta)_2$ lobes, the β subunits must compose that bridged core.

Thus, based on the results herein, we can now conclude that the phospho-activated PhK complex, similar to the Ca^{2+}-activated form, also demonstrates significant structural changes in the region of its bridges. β-Dimers and higher order oligomers containing two or more copies of this subunit were detected only in spectra of phospho-PhK (either intact or solution disrupted), revealing significant differences in the subunit interaction patterns between the nonactivated and phospho-activated conformers (Fig. 5). The self-interactions of β indicated by the detection of β_2, $\alpha\beta_2$, $\alpha\beta_3\delta$, and $\beta_4\delta_2$ subcomplexes only in phospho-activated PhK are consistent with our previous yeast two-hybrid screens showing that self-interaction of the β subunit is greatly enhanced by mutation of its known N-terminal phosphorylatable regulatory serines to phosphomimetic glutamates (33). The β subunit is predominant in the regulation of PhK by phosphorylation (33), in that its phosphorylation parallels activation of the catalytic kinase γ subunit in the complex (59, 60). The phosphorylation of PhK has also been reported to reduce its stringency for activation by Ca^{2+} (20), and a linkage between β and the Ca^{2+}-binding δ subunit is seen in the $\beta\delta$ and $\beta_4\delta_2$ subcomplexes observed in spectra of intact and solution disrupted forms of phospho-PhK. Moreover, detection of the $\alpha\beta\gamma\delta$ protomer in the phospho-activated conformer of PhK suggests that β is simultaneously able to maintain interprotomeric contacts with adjacent β subunits and intraprotomeric contacts with the α, γ, and δ subunits. Our models of nonactivated and phospho-activated PhK depicted in Fig. 5 show for the first time in a global context the architecture of subunit interactions in each conformer and the changes induced in the subunit interaction pattern upon phosphorylation.

* Supported by NIH grant DK32953 (to GMC) and the Royal Society and the Engineering and Physical Science Research Council (to CVR).

S This article contains supplemental Figs. S1 to S3.

** To whom correspondence should be addressed: E-mail: carol.robinson@chem.ox.ac.uk; Tel.: +44 (0)1865 275473.

REFERENCES

1. Krebs, E. G., and Fischer, E. H. (1956) The phosphorylase b to a converting enzyme of rabbit skeletal muscle. *Biochim. Biophys. Acta* **20,** 150–157
2. Brushia, R. J., and Walsh, D. A. (1999) Phosphorylase kinase: the complexity of its regulation is reflected in the complexity of its structure. *Front. Biosci.* **4,** D618–D641
3. Priddy, T. S., MacDonald, B. A., Heller, W. T., Nadeau, O. W., Trewhella, J., and Carlson, G. M. (2005) Ca2+-induced structural changes in phosphorylase kinase detected by small-angle X-ray scattering. *Protein Sci.* **14,** 1039–1048
4. Nadeau, O. W., Carlson, G. M., and Gogol, E. P. (2002) A Ca(2+)-dependent global conformational change in the 3D structure of phosphorylase kinase obtained from electron microscopy. *Structure* **10,** 23–32
5. Nadeau, O. W., Gogol, E. P., and Carlson, G. M. (2005) Cryoelectron microscopy reveals new features in the three-dimensional structure of phosphorylase kinase. *Protein Sci.* **14,** 914–920
6. Venien-Bryan, C., Jonic, S., Skamnaki, V., Brown, N., Bischler, N., Oikonomakos, N. G., Boisset, N., and Johnson, L. N. (2009) The structure of phosphorylase kinase holoenzyme at 9.9 angstroms resolution and location of the catalytic subunit and the substrate glycogen phosphorylase. *Structure* **17,** 117–127
7. Venien-Bryan, C., Lowe, E. M., Boisset, N., Traxler, K. W., Johnson, L. N., and Carlson, G. M. (2002) Three-dimensional structure of phosphorylase kinase at 22 A resolution and its complex with glycogen phosphorylase b. *Structure* **10,** 33–41
8. Traxler, K. W., Norcum, M. T., Hainfeld, J. F., and Carlson, G. M. (2001) Direct visualization of the calmodulin subunit of phosphorylase kinase via electron microscopy following subunit exchange. *J. Struct. Biol.* **135,** 231–238
9. Wilkinson, D. A., Marion, T. N., Tillman, D. M., Norcum, M. T., Hainfeld, J. F., Seyer, J. M., and Carlson, G. M. (1994) An epitope proximal to the carboxyl terminus of the alpha-subunit is located near the lobe tips of the phosphorylase kinase hexadecamer. *J. Mol. Biol.* **235,** 974–982
10. Wilkinson, D. A., Norcum, M. T., Fizgerald, T. J., Marion, T. N., Tillman, D. M., and Carlson, G. M. (1997) Proximal regions of the catalytic gamma and regulatory beta subunits on the interior lobe face of phosphorylase kinase are structurally coupled to each other and with enzyme activation. *J. Mol. Biol.* **265,** 319–329
11. Norcum, M. T., Wilkinson, D. A., Carlson, M. C., Hainfeld, J. F., and Carlson, G. M. (1994) Structure of phosphorylase kinase. A three-dimensional model derived from stained and unstained electron micrographs. *J. Mol. Biol.* **241,** 94–102
12. Heilmeyer, L. M., Jr. (1991) Molecular basis of signal integration in phosphorylase kinase. *Biochim. Biophys. Acta* **1094,** 168–174
13. Cohen, P., Burchell, A., Foulkes, J. G., and Cohen, P. T. (1978) Identification of the Ca2+-dependent modulator protein as the fourth subunit of rabbit skeletal muscle phosphorylase kinase. *FEBS Lett.* **92,** 287–293
14. Dasgupta, M., Honeycutt, T., and Blumenthal, D. K. (1989) The gamma-subunit of skeletal muscle phosphorylase kinase contains two noncontiguous domains that act in concert to bind calmodulin. *J. Biol. Chem.* **264,** 17156–17163
15. Jeyasingham, M. D., Artigues, A., Nadeau, O. W., and Carlson, G. M. (2008) Structural evidence for co-evolution of the regulation of contraction and energy production in skeletal muscle. *J. Mol. Biol.* **377,** 623–629
16. Meyer, W. L., Fischer, E. H., and Krebs, E. G. (1964) Activation of skeletal muscle phosphorylase b kinase by Ca. *Biochemistry* **3,** 1033–1039
17. Kilimann, M. W., Zander, N. F., Kuhn, C. C., Crabb, J. W., Meyer, H. E., and Heilmeyer, L. M., Jr. (1988) The alpha and beta subunits of phosphorylase kinase are homologous: cDNA cloning and primary structure of the beta subunit. *Proc. Natl. Acad. Sci. U.S.A.* **85,** 9381–9385
18. Wullrich, A., Hamacher, C., Schneider, A., and Kilimann, M. W. (1993) The multiphosphorylation domain of the phosphorylase kinase alpha M and alpha L subunits is a hotspot of differential mRNA processing and of molecular evolution. *J. Biol. Chem.* **268,** 23208–23214
19. Burger, D., Cox, J. A., Fischer, E. H., and Stein, E. A. (1982) The activation of rabbit skeletal muscle phosphorylase kinase requires the binding of 3 Ca2+ per delta subunit. *Biochem. Biophys. Res. Commun.* **105,** 632–638
20. Cohen, P. (1980) The role of calcium ions, calmodulin and troponin in the regulation of phosphorylase kinase from rabbit skeletal muscle. *Eur. J. Biochem.* **111,** 563–574
21. Heilmeyer, L. M., Jr., Meyer, F., Haschke, R. H., and Fischer, E. H. (1970) Control of phosphorylase activity in a muscle glycogen particle. II. Activation by calcium. *J. Biol. Chem.* **245,** 6649–6656
22. Kilimann, M. W., and Heilmeyer, L. M., Jr. (1982) Multiple activities on phosphorylase kinase. 1. Characterization of three partial activities by their response to calcium ion, magnesium ion, pH, and ammonium chloride and effect of activation by phosphorylation and proteolysis. *Biochemistry* **21,** 1727–1734

23. Brostrom, C. O., Hunkeler, F. L., and Krebs, E. G. (1971) The regulation of skeletal muscle phosphorylase kinase by Ca2+. *J. Biol. Chem.* **246,** 1961–1967
24. Pickett-Gies, C. A., and Walsh, D. A. (1986) Phosphorylase kinase. In *The Enzymes* (Boyer, P. D., and Krebs, E. G., eds) 3rd Ed., pp. 395–459, Academic Press, Orlando, FL
25. Nadeau, O. W., and Carlson, G. M. (2012) A review of methods used for identifying structural changes in a large protein complex. *Methods Mol. Biol.* **796,** 117–132
26. Liu, W., Priddy, T. S., and Carlson, G. M. (2008) Physicochemical changes in phosphorylase kinase associated with its activation. *Protein Sci.* **108,** 2111–2119
27. Priddy, T. S., Middaugh, C. R., and Carlson, G. M. (2007) Electrostatic changes in phosphorylase kinase induced by its obligatory allosteric activator Ca2+. *Protein Sci.* **16,** 517–527
28. Priddy, T. S., Price, E. S., Johnson, C. K., and Carlson, G. M. (2007) Single molecule analyses of the conformational substates of calmodulin bound to the phosphorylase kinase complex. *Protein Sci.* **16,** 1017–1023
29. Ayers, N. A., Nadeau, O. W., Read, M. W., Ray, P., and Carlson, G. M. (1998) Effector-sensitive cross-linking of phosphorylase b kinase by the novel cross-linker 4-phenyl-1,2,4-triazoline-3,5-dione. *Biochem. J.* **331,** 137–141
30. Nadeau, O. W., Sacks, D. B., and Carlson, G. M. (1997) The structural effects of endogenous and exogenous Ca2+/calmodulin on phosphorylase kinase. *J. Biol. Chem.* **272,** 26202–26209
31. Nadeau, O. W., Traxler, K. W., Fee, L. R., Baldwin, B. A., and Carlson, G. M. (1999) Activators of phosphorylase kinase alter the cross-linking of its catalytic subunit to the C-terminal one-sixth of its regulatory alpha subunit. *Biochemistry* **38,** 2551–2559
32. Rice, N. A., Nadeau, O. W., Yang, Q., and Carlson, G. M. (2002) The calmodulin-binding domain of the catalytic gamma subunit of phosphorylase kinase interacts with its inhibitory alpha subunit: evidence for a Ca2+ sensitive network of quaternary interactions. *J. Biol. Chem.* **277,** 14681–14687
33. Nadeau, O. W., Anderson, D. W., Yang, Q., Artigues, A., Paschall, J. E., Wyckoff, G. J., McClintock, J. L., and Carlson, G. M. (2007) Evidence for the location of the allosteric activation switch in the multisubunit phosphorylase kinase complex from mass spectrometric identification of chemically crosslinked peptides. *J. Mol. Biol.* **365,** 1429–1445
34. Trempe, M. R., and Carlson, G. M. (1987) Phosphorylase kinase conformers. Detection by proteases. *J. Biol. Chem.* **262,** 4333–4340
35. Fitzgerald, T. J., and Carlson, G. M. (1984) Activated states of phosphorylase kinase as detected by the chemical cross-linker 1,5-difluoro-2,4-dinitrobenzene. *J. Biol. Chem.* **259,** 3266–3274
36. Carlson, G. M. (1984) Precautions when determining kinetically the order of inactivation of enzymes by functionally irreversible inhibitors. *Biochim. Biophys. Acta* **789,** 347–350
37. Nadeau, O. W., Sacks, D. B., and Carlson, G. M. (1997) Differential affinity cross-linking of phosphorylase kinase conformers by the geometric isomers of phenylenedimaleimide. *J. Biol. Chem.* **272,** 26196–26201
38. Nadeau, O. W., and Carlson, G. M. (1994) Zero length conformation-dependent cross-linking of phosphorylase kinase subunits by transglutaminase. *J. Biol. Chem.* **269,** 29670–29676
39. Nadeau, O. W., and Carlson, G. M. (2005) Protein interactions captured by chemical cross-linking. In *Protein-Protein Interactions: A Molecular Cloning Manual* (Golemis, E., and Adams, P. D., eds) 2nd Ed., pp. 105–127, Cold Spring Harbor Laboratory Press, Cold Spring Harbor, NY
40. Benesch, J. L., Ruotolo, B. T., Simmons, D. A., and Robinson, C. V. (2007) Protein complexes in the gas phase: technology for structural genomics and proteomics. *Chem. Rev.* **107,** 3544–3567
41. Hernandez, H., and Robinson, C. V. (2007) Determining the stoichiometry and interactions of macromolecular assemblies from mass spectrometry. *Nat. Protoc.* **2,** 715–726
42. Sobott, F., Hernandez, H., McCammon, M. G., Tito, M. A., and Robinson, C. V. (2002) A tandem mass spectrometer for improved transmission and analysis of large macromolecular assemblies. *Anal. Chem.* **74,** 1402–1407
43. King, M. M., and Carlson, G. M. (1981) Synergistic activation by Ca2+ and Mg2+ as the primary cause for hysteresis in the phosphorylase kinase reactions. *J. Biol. Chem.* **256,** 11058–11064
44. Hernandez, H., Dziembowski, A., Taverner, T., Seraphin, B., and Robinson, C. V. (2006) Subunit architecture of multimeric complexes isolated directly from cells. *EMBO Rep.* **7,** 605–610
45. Taverner, T., Hernandez, H., Sharon, M., Ruotolo, B. T., Matak-Vinkovic, D., Devos, D., Russell, R. B., and Robinson, C. V. (2008) Subunit architecture of intact protein complexes from mass spectrometry and homology modeling. *Acc. Chem. Res.* **41,** 617–627
46. McKay, A. R., Ruotolo, B. T., Ilag, L. L., and Robinson, C. V. (2006) Mass measurements of increased accuracy resolve heterogeneous populations of intact ribosomes. *J. Am. Chem. Soc.* **128,** 11433–11442
47. Aebersold, R., and Mann, M. (2003) Mass spectrometry-based proteomics. *Nature* **422,** 198–207
48. Chan, K. F., and Graves, D. J. (1982) Isolation and physicochemical properties of active complexes of rabbit muscle phosphorylase kinase. *J. Biol. Chem.* **257,** 5939–5947
49. Chan, K. F., and Graves, D. J. (1982) Rabbit skeletal muscle phosphorylase kinase. Catalytic and regulatory properties of the active alpha gamma delta and gamma delta complexes. *J. Biol. Chem.* **257,** 5948–5955
50. Burchell, A., Cohen, T. W., and Cohen, P. (1976) Distribution of isoenzymes of the glycogenolytic cascade in different types of muscle fibre. *FEBS Lett.* **67,** 17–22
51. Jennissen, H. P., and Heilmeyer, L. M., Jr. (1974) Multiple forms of phosphorylase kinase in red and white skeletal muscle. *FEBS Lett.* **42,** 77–80
52. Harmann, B., Zander, N. F., and Kilimann, M. W. (1991) Isoform diversity of phosphorylase kinase alpha and beta subunits generated by alternative RNA splicing. *J. Biol. Chem.* **266,** 15631–15637
53. Cheng, A., Fitzgerald, T. J., and Carlson, G. M. (1985) Adenosine 5′-diphosphate as an allosteric effector of phosphorylase kinase from rabbit skeletal muscle. *J. Biol. Chem.* **260,** 2535–2542
54. Paudel, H. K., and Carlson, G. M. (1987) Inhibition of the catalytic subunit of phosphorylase kinase by its alpha/beta subunits. *J. Biol. Chem.* **262,** 11912–11915
55. Paudel, H. K., and Carlson, G. M. (1990) The quaternary structure of phosphorylase kinase as influenced by low concentrations of urea. Evidence suggesting a structural role for calmodulin. *Biochem. J.* **268,** 393–399
56. Benesch, J. L., and Robinson, C. V. (2006) Mass spectrometry of macromolecular assemblies: preservation and dissociation. *Curr. Opin. Struct. Biol.* **16,** 245–251
57. Trempe, M. R., Carlson, G. M., Hainfeld, J. F., Furcinitti, P. S., and Wall, J. S. (1986) Analyses of phosphorylase kinase by transmission and scanning transmission electron microscopy. *J. Biol. Chem.* **261,** 2882–2889
58. Boulatnikov, I. G., Peters, J. L., Nadeau, O. W., Sage, J. M., Daniels, P. J., Kumar, P., Walsh, D. A., and Carlson, G. M. (2009) Expressed phosphorylase b kinase and its alphagammadelta subcomplex as regulatory models for the rabbit skeletal muscle holoenzyme. *Biochemistry (Mosc.)* **48,** 10183–10191
59. King, M. M., Fitzgerald, T. J., and Carlson, G. M. (1983) Characterization of initial autophosphorylation events in rabbit skeletal muscle phosphorylase kinase. *J. Biol. Chem.* **258,** 9925–9930
60. Ramachandran, C., Goris, J., Waelkens, E., Merlevede, W., and Walsh, D. A. (1987) The interrelationship between cAMP-dependent alpha and beta subunit phosphorylation in the regulation of phosphorylase kinase activity. Studies using subunit specific phosphatases. *J. Biol. Chem.* **262,** 3210–3218